Pol. J. Environ. Stud. Vol. XX, No. X (XXXX), 1-21
DOI: *10.15244/pjoes/219751* ONLINE PUBLICATION DATE: 2026-07-10

Original Research

Spatiotemporal Evolution and Multi-Scenario Simulation of Trade-offs between Ecosystem Services: A Case Study of Nansi Lake Basin, China

Jie Zhao[1]*, Xu Jiang[1], Cheng Li[2]

[1]School of Geomatics, Geography and Urban-Rural Planning, Jiangsu Normal University
[2]School of Architecture and Design, China University of Mining and Technology

Received: 18 December 2025
Accepted: 18 March 2026

Abstract

Analyzing trade-offs/synergies among ecosystem services is essential for promoting ecological conservation and socio-economic development, thereby enhancing comprehensive human well-being. Taking the Nansi Lake Basin as the study area, this research reveals the spatiotemporal dynamics of service couplings and their spatiotemporal distribution over the period from 2000 to 2020. A Geographically Weighted Regression Random Forest (GWRF) model was employed to investigate the effects of influencing factors on these interrelationships. Furthermore, the GeoSOS-FLUS model was utilized to simulate future linkages under three different scenarios by the year 2040. The findings indicate that ecosystem services exhibited significant spatial heterogeneity, with water retention and grain production services showing consistent annual increments. The trade-off/synergy relationships among ecosystem services experienced complex dynamic changes. Key influencing factors included natural elements such as elevation, annual precipitation, and evapotranspiration. The effects of all factors on service balances were spatially heterogeneous. The relationships among ecosystem services differed markedly across the development scenarios. Under the natural development scenario, services demonstrated synergistic co-development with low trade-off levels. The ecological conservation scenario enhanced water purification services while maintaining the stability of grain production services, resulting in relatively stable interaction dynamics. In contrast, the economic development scenario led to a general decline in ecosystem services, revealing prominent conflicts among them.

Keywords: Nansi Lake basin, ecosystem services, trade-off relationships, geographically weighted regression random forest model, multi-scenario simulation

*e-mail: jiezhao@jsnu.edu.cn

Introduction

Ecosystem services constitute the natural environmental conditions and benefits formed and provided by ecosystems for human survival. They establish a critical linkage between human society and the natural environment, delivering diverse products essential for human existence and development [1, 2]. In 1997, Costanza et al. [3] conducted a global quantitative assessment of ecosystem service values, highlighting their critical importance to human well-being. With ongoing population growth and rising living standards, the products provided by ecosystem services have become insufficient to meet the demand [4]. Concurrently, human impacts on the ecological environment have grown more direct and severe, as obtaining targeted products often comes at the expense of other ecosystem services [5], triggering serious ecological and environmental issues such as water scarcity, soil erosion, environmental pollution, and land degradation. China is currently at a turning point in its environmental strategy, moving away from simple local fixes toward a more systematic approach to ecological governance and low-carbon growth [6]. Furthermore, the United Nations Millennium Ecosystem Assessment Report indicates that ecosystem service functions face severe threats [7]. Consequently, research on the functional balances among ecosystem services has become a prominent focus, holding significant implications for promoting ecosystem stability and sustainable development.

Significant progress has been made in understanding the interdependencies between ecosystem services [8]. Various quantitative methodologies, particularly multi-scenario simulations and correlation analysis [9, 10], have been extensively employed to disentangle these complex trade-offs and synergies. However, existing research remains largely qualitative, with limited capacity to quantify the intensity of these interactions, and spatial heterogeneity is difficult to visualize. Regarding the underlying drivers and mechanisms behind these ecological tensions, methods such as principal component analysis, geographic detectors, and regression analysis have been employed. For instance, Jackson et al. applied a multi-criteria analysis to demonstrate that identifying priority ecosystem services is essential for tidal wetland restoration, precisely because their benefits and demand exhibit pronounced spatial heterogeneity [11]. However, such heterogeneity often creates overlapping regions of synergy and trade-offs, making simple visualization difficult. To address this, the GWRF model, first proposed in 2019 [12], can uncover complex nonlinear relationships in data while elucidating the local effects of variables [13]. The application of a random forest model by Chen et al. enabled the quantification of ecosystem service trade-offs and the identification of their key drivers in the Qionglai-Daxiangling region over the period 1990-2020 [14]. Recent studies have further extended these capabilities by employing the GWRF model to assess regional carbon storage and ecosystem drivers, demonstrating its robust application potential [15]. While these methods partially reveal how services interact, they exhibit limitations in representing the spatial heterogeneity of dynamic changes and capturing complex nonlinear relationships [16]. The core of spatiotemporal dynamic simulation of ecosystem services lies in uncovering evolution patterns, typically focusing on land-use transitions and anthropogenic activities as primary drivers [17]. Additionally, scenario simulation serves as a primary tool for analyzing future dynamics. For instance, multi-scenario projections of ecosystem service values have highlighted the differential impacts of varying development strategies on ecosystem management [18]. Recent assessments utilizing integrated models have revealed significant variations in ecosystem service provisioning under diverse future pathways [19]. A prevailing limitation in multi-scenario simulation analysis is the difficulty in accurately predicting and interpreting the trade-offs among future ecosystem services [20]. Many studies employ relatively simplified scenario settings that fail to integrate regional realities fully. Most research merely compares total ecosystem service changes across scenarios without delving into the evolution of trade-off relationships. This study combines the localized ecological context with a specific analysis of how service interdependencies transform under different scenarios.

The Nansi Lake Basin serves as a vital water conveyance channel and regulating reservoir for China's East Route Project of the South-to-North Water Diversion. Ecological conservation in the Nansi Lake Basin is of great significance and is closely linked to socioeconomic development. However, in recent years, the basin has faced ecological challenges, where issues such as overexploitation of resources and environmental degradation have significantly impacted its ecosystem services [21]. Given this context, this study focuses on the Nansi Lake Basin. Integrating multi-source data, it employs the InVEST model to analyze the spatiotemporal patterns of seven ecosystem services: water retention, soil conservation, water purification, carbon storage, water yield, grain production, and net primary productivity. Subsequently, Pearson correlation analysis and Root Mean Square Error (RMSE) are used to reveal trade-off relationships among these services. The GWRF model is employed to investigate factors influencing these relationships. Finally, a more comprehensive scenario is constructed, integrating natural and socioeconomic factors to conduct an in-depth analysis of the spatiotemporal evolution of ecosystem service balances in the study area. This provides a scientific basis for ecological conservation and sustainable development in the Nansi Lake Basin.

Materials and Methods

Study Area

The Nansi Lake Basin, located in the southwestern part of Shandong Province, represents the largest lake system within the province, encompassing four major lakes: Nanyang Lake, Dushan Lake, Weishan Lake, and Zhaoyang Lake. This basin extends across Shandong and Jiangsu provinces, covering Jining, Heze, Tai'an, Zaozhuang, and Xuzhou cities. With a total area of approximately 31,000 km^2, the basin is characterized by a temperate continental monsoon climate and exhibits a topographical gradient that is higher in the east and lower in the west (Fig. 1). A network of 53 rivers traverses the basin, all of which play vital roles in transportation, ecological conservation, and water regulation. These waterways function as key transmission channels and storage hubs for the Eastern Route of the South-to-North Water Diversion Project. However, the basin faces significant constraints on ecological conservation, primarily stemming from cross-regional economic disparities, intensive land resource exploitation, and inconsistent governance frameworks [22]. Currently, multiple pressures are driving a marked ecological imbalance. Recurring droughts, declining vegetation coverage, and unsustainable land use practices are accelerating environmental degradation in the region [23]. Therefore, conducting an in-depth investigation into the evolution of trade-offs in ecosystem services within the Nansi Lake Basin and elucidating the interrelationships among influencing factors will not only bolster ecological conservation efforts in the region but also furnish a scientific basis and decision support for the basin's high-quality development.

Data Source

The datasets utilized in this study are summarized as follows: (1) Land use/cover data for 2000, 2010, and 2020 were obtained from the Resource and Environment Science and Data Center of the Chinese Academy of Sciences (https://www.resdc.cn). These datasets possess a spatial resolution of 30 meters and classify land use, including arable land, forest land, grassland, water bodies, construction land, and unutilized land. (2) Administrative boundary data sourced from the National Basic Geographic Database (http://www.ngcc.cn/ngcc/), specifically county-level boundary data for Shandong, Jiangsu, Anhui, and Henan provinces. (3) Meteorological data, including temperature, precipitation, and evapotranspiration data sourced from the China Meteorological Data Network (http://data.cam.cn), with a spatial resolution of 1 km. (4) Soil property data were obtained from the China Soil Dataset within the World Soil Database (http://gaes.fao.org/pages/hwsd), with a spatial resolution of 1 km. (5) Elevation data sourced from the Geospatial Data Cloud Platform (http://www.gscloud.cn/), with a spatial resolution of 30 m. (6) Gross Domestic Product (GDP) data were compiled from China's GDP Spatial Distribution Kilometer Grid Dataset and the China Urban Statistical Yearbook. (7) Population density data were retrieved from WorldPop (https://www.worldpop.org), at a spatial resolution of 1 km. (8) Human Footprint Index data were sourced from (https://geoservice.dlr.de), with a spatial resolution of 1 km. All spatial datasets were uniformly projected to the WGS_1984_UTM_Zone_50N coordinate system using ArcGIS 10.7 to ensure consistency in spatial analysis. (9) Additional elevation data were also obtained from the Geospatial Data Cloud

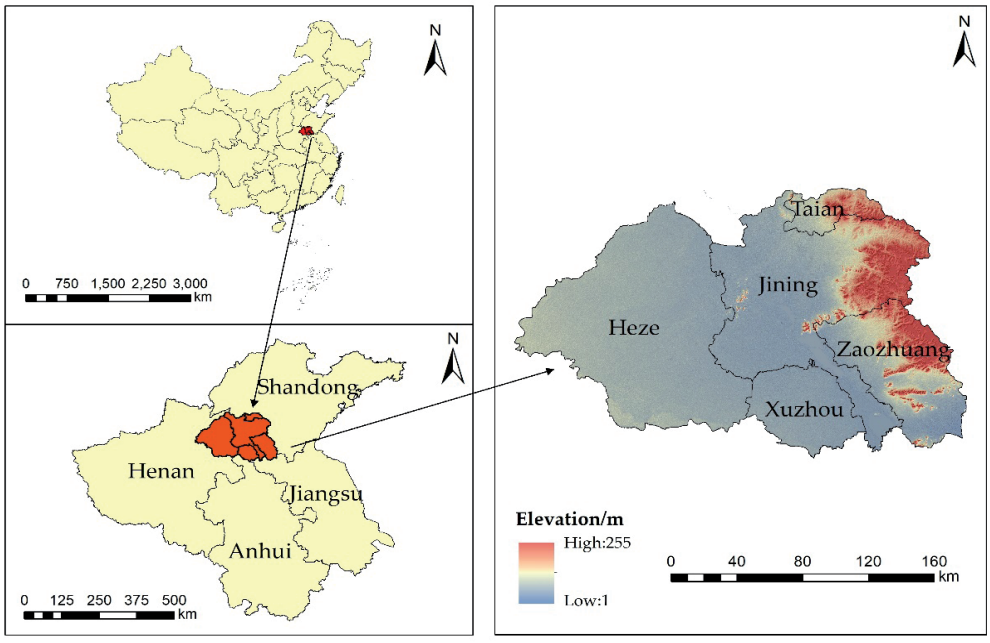

Fig. 1. Location map of the research area.

(http://www.gscloud.cn/). (10) Socioeconomic statistics were collected from provincial and municipal statistical yearbooks covering the period 2001–2021.

Research Methods

Ecosystem Services Assessment

1. Water Yield

Water yield is quantified using the InVEST Water Yield module, which is grounded in the water balance principle and the Budyko hydrological framework to simulate the partitioning of precipitation into evapotranspiration and runoff [24]. Water yield is quantified using the water balance approach integrated into the InVEST model. Within a grid cell, water yield equals precipitation minus actual evapotranspiration. The specific calculation formula is as follows:

$$Y_x = \left(1 - \frac{AET_x}{P_x}\right) \times P_x \tag{1}$$

where Y_x is annual water yield (mm) for grid cell x; AET_x is actual evapotranspiration (mm) for grid cell x; P_x is precipitation (mm) for grid cell x.

2. Water Retention

The water retention service in this study is evaluated by refining the output of the InVEST Water Yield module. Since the standard InVEST model primarily provides total annual water yield (Y), we further integrated the topographic index (TI), velocity coefficient, and soil saturated hydraulic conductivity (K_{sat}) to more accurately reflect the ecosystem's capacity to intercept and store water.

This methodological framework follows the established approach used in recent peer-reviewed studies on watershed-scale water conservation [25]. The water retention function reflects the capacity of a watershed's ecosystem to conserve moisture. The water retention volume is calculated as follows:

$$WR = Min\left(1, \frac{249}{Velocity}\right) \times Min\left(1, \frac{0.9 \times TI}{3}\right) \times Min\left(1, \frac{K_{sat}}{300}\right) \times Y \tag{2}$$

where WR is the water retention (mm); $Velocity$ is the velocity coefficient; TI is the topographic index; K_{sat} is the saturated soil conductivity (cm/d); Y is the water yield (mm) calculated by the InVEST model (Eq. (1)).

3. Soil Conservation

The sediment delivery ratio module within the InVEST model calculates soil conservation quantities. The soil conservation service in this study is quantified using the Sediment Delivery Ratio (SDR) module of the InVEST model. This approach enhances the traditional Revised Universal Soil Loss Equation (RUSLE) by accounting for the spatial processes of sediment transport and the filtration capacity of downstream vegetation. By integrating topographical features with soil erodibility and rainfall erosivity factors, this model provides a more spatially explicit assessment of soil retention [26]. Based on the principles of the Revised Universal Soil Loss Equation, it incorporates upstream sediment interception and vegetation protection against soil erosion, yielding more scientific and precise results. Soil actual erosion is calculated by integrating vegetation cover and corresponding soil conservation measures, while soil potential erosion represents erosion levels without these factors. The difference between the two values represents the soil conservation service. The specific calculations are performed using the following equations:

$$RKLS = R \times K \times LS \tag{3}$$

$$USLE = R \times K \times LS \times P \times C \tag{4}$$

$$SD = RKLS - USLE \tag{5}$$

where $USLE$ denotes the actual soil erosion, t/(hm²·a); $RKLS$ represents potential soil erosion, t/(hm²·a); SD denotes soil conservation amount, t/(hm²·a); R represents rainfall erosion potential factor, MJ·mm/(hm²·h·a); K is soil erodibility factor, t·hm²·h/ (MJ·hm²·mm); LS is slope length factor; P is the soil and water retention measure factor; C is the vegetation cover and management factor.

4. Water Purification

The water purification service in this study is evaluated using the Nutrient Delivery Ratio (NDR) module of the InVEST model. This module simulates the biophysical processes of nutrient transport by calculating the nutrient load contribution of each grid cell and its subsequent retention by downstream vegetation. By incorporating the hydrological sensitivity of the landscape and the filtration capacity of different land use types, this approach provides a more robust representation of nitrogen (N) and phosphorus (P) removal than traditional export coefficient methods [27]. Vegetation and soil purify water by removing or reducing nutrient pollutants in runoff through storage and conversion processes. The calculations are performed as follows:

$$ALV_x = HSS_x \times pol_x \tag{6}$$

$$HSS_x = \frac{\lambda_x}{\lambda_w} \tag{7}$$

$$\lambda_x = \log(\Sigma_u Y_u) \tag{8}$$

where ALV_x is the load value adjusted at grid cell x; pol_x is the output coefficient for grid cell x; HSS_x is the hydrological sensitivity score for grid cell x. λ_x denotes the runoff index for grid cell x; λ_w represents the average runoff index for the catchment; $\Sigma_u Y_u$ signifies the sum of water contributions from upstream grid cells along the runoff path to grid cell x.

5. Carbon Storage

The carbon storage service in this study is quantified using the Carbon Storage and Sequestration module of the InVEST model. This module estimates the total carbon stock by integrating land use/land cover (LULC) maps with four fundamental carbon pools: above-ground biomass, below-ground biomass, soil organic matter, and dead organic matter. This methodological framework is widely utilized for assessing the impacts of regional land management and ecosystem shifts on carbon sequestration capacity [28]. The carbon storage module in the InVEST model calculates carbon storage under land cover scenarios based on land use data and four fundamental carbon pools. The specific calculation formula is as follows:

$$C_{tot} = C_{above} + C_{below} + C_{soil} + C_{dead} \quad (9)$$

where C_{tot} is the total carbon storage; C_{above} is the above-ground biotic carbon storage; C_{belov} is the below-ground biotic carbon storage; C_{soil} is the soil carbon storage; C_{dead} is the dead organic carbon storage.

6. Grain Production

A significant linear correlation exists between crop yield and the Normalized Difference Vegetation Index (NDVI), as NDVI serves as a sensitive indicator of crop photosynthesis and biomass accumulation. This study extracts the maximum NDVI value for a given year to spatially distribute grain production data. Based on this, grain yield is assessed by allocating the total grain production to cultivated grid cells according to their NDVI values. This grid-based approach effectively captures pixel-level heterogeneity in agricultural productivity and has been validated as a robust method for crop yield monitoring across diverse landscapes in China [29]. The specific calculation formula is as follows:

$$Crop_x = \frac{NDVI_x}{NDVI_{sum}} \times Crop_{sum} \quad (10)$$

where $Crop_x$ is Grain yield allocated to farmland grid x, $Crop_{sum}$ is the total grain yield for a county unit $NDVI_x$ is the maximum NDVI value for grid unit x in a given year $NDVI_{sum}$ is the sum of NDVI values for all farmland grids in a county unit.

7. Net Primary Productivity

This study employs the Carnegie-Ames-Stanford Approach (CASA) photosynthetic efficiency model to calculate ecosystem net primary productivity. The CASA model is an established light-use efficiency framework that integrates remote sensing and meteorological data, providing a robust approach for quantifying the carbon sequestration capacity of terrestrial ecosystems [30]. The calculation formula is as follows:

$$NPP_{x,t} = APAR_{x,t} \times \varepsilon_{x,t} \quad (11)$$

where $NPP_{x,t}$ represents the net primary productivity ($t \cdot ha^{-1} \cdot yr^{-1}$) of vegetation on grid x during month t, determined by the product of photosynthetically active radiation (APAR) absorbed by vegetation and the photosynthetic efficiency $\varepsilon_{x,t}$. $APAR_{x,t}$ represents the photosynthetically active radiation absorbed by vegetation on grid cell x during month t (MJ/m^2); $\varepsilon_{x,t}$ denotes the actual photosynthetic efficiency of vegetation on grid cell x during month t ($g \cdot C \cdot MJ^{-1}$).

Assessment of Trade-offs of Ecosystem Services

1. Pearson Correlation Analysis

Pearson correlation analysis was employed to quantify trade-offs and synergies among ecosystem services [31]. This approach is a standard method for identifying the direction and strength of interactions, allowing for a clear distinction between antagonistic and mutually beneficial relationships. Furthermore, grid-scale calculation effectively captures the spatiotemporal heterogeneity of these interactions, providing a scientific basis for differentiated spatial management [32]. The formula is as follows:

$$r = \frac{\Sigma i\left(x_{ij} - \bar{x}\right)\left(y_{ij} - \bar{y}\right)}{\sqrt{\Sigma \mathrm{i}\left(x_{ij} - \bar{x}\right)^2 \Sigma \mathrm{i}\left(y_{ij} - y\right)^2}} \quad (12)$$

where r is the correlation coefficient; x_{ij} and y_{ij} represent data values for different ecosystem services; $\bar{x}$ and $\bar{y}$ denote the mean values of x_{ij} and y_{ij}, respectively. The range of r is [-1, 1]. A positive r indicates a synergistic relationship, while a negative r indicates a trade-off relationship.

2. Root Mean Square Error

RMSE was calculated to quantify the magnitude of trade-offs among multiple ecosystem services. Calculating the RMSE between ecosystem services quantifies the trade-offs among multiple service types, thereby elucidating complex trade-off relationships and providing refined spatial heterogeneity information [33]. This metric is particularly effective in identifying the imbalance between services, where a higher RMSE indicates a more intense trade-off and more pronounced spatial conflicts between different ecological functions [34]. The calculation formula is as follows:

$$EST = \sqrt{\frac{1}{n-1}\sum_{i=1}^{n}(ES_i - \overline{ES})^2} \quad (13)$$

where EST represents the RMSE of n ecosystem services, ES_i denotes the normalized value of the i-th ecosystem service, and $\overline{ES}$ is the average value of the n ecosystem services.

Geographically Weighted Random Forest Model

Random forest is an ensemble machine learning method founded on classification trees. It is not significantly affected by multicollinearity issues and maintains relatively stable and reliable performance when handling data with missing values and imbalanced datasets [35]. By incorporating a spatially explicit framework [36], the GWRF model integrates the advantages of both random forest models and geographically weighted regression, enabling more precise predictions for each geographic location's observed values [37]. This approach has been proven effective for capturing spatial nonstationarity in recent ecological driver analyses, with final local estimates obtained through a spatially weighted voting or aggregation mechanism [38, 39]. Based on the random forest model, the GWRF model can be formally expressed as follows:

$$Y_i = a(u_i, v_i)x_i + e \tag{14}$$

where $a(u_i, v_i)x_i$ represents the spatially calibrated prediction value of the random forest model at location (u_i, v_i).

The relative importance of each driver factor to the trade-off synergies of ecosystem services is expressed as the percentage increase in mean squared error (%IncMSE), calculated as follows:

$$R_i = \frac{I_i}{\sum_{i=1}^{n} I_i} \tag{15}$$

where R_i denotes the relative importance of the driver factor i, I_i represents the increase in mean squared error for the driver factor i, and n is the total number of driver factors.

Multi-Scenario Simulation of Ecosystem Services

The FLUS model is a powerful tool for simulating land use change and predicting future scenarios. By building upon the iterative simulation logic for multi-type land use competition [40], it can be applied to analyses such as land use change simulation, urban-rural development simulation, ecosystem management, national spatial planning, regional land suitability, and landscape pattern evolution. This sophisticated simulation framework, derived from Cellular Automata (CA), is specifically designed to capture the trade-offs between natural processes and human activities in shaping land use patterns [41]. To implement this, leveraging the integrated ANN-CA architecture recently applied in river basin ecological assessment [42], Artificial Neural Network (ANN) algorithms were first employed to calculate the occurrence probability of various land types. Subsequently, Markov chains and CA models were integrated to project future patterns, with accuracy validation performed to ensure the model's robustness and applicability [43]. This study utilized the GeoSOS-FLUS model to simulate and predict land use patterns in the Nansi Lake Basin, modeling the land use configurations under three scenarios for the study area in 2040: natural development, ecological conservation, and economic development.

Natural Development Scenario: Serving as a baseline comparison, this scenario assumes that land use development structures and patterns evolve without external interference, driven solely by historical trend inertia to predict outcomes [44]. Land use areas and driving factor data align with historical trends in this scenario.

Ecological Conservation Scenario: To enhance prediction accuracy, the transition matrix and sector weights were modified. Guided by the ecological security constraints [45], this scenario prioritizes restricting the conversion of forest, grassland, and water bodies to construction land or cultivated land (transition potential set to 0). Conversely, the conversion of cultivated land to water bodies was encouraged (set to 1) to simulate ecological restoration.

Economic Development Scenario: This scenario adopts a production-oriented approach that prioritizes economic growth. Guided by the balance between urban expansion and agricultural sustainability in the Huaihe River Basin, cultivated land is designated as a restricted conversion type [46]. To maintain the agricultural base, all land types except construction land are permitted to convert into farmland, ensuring the "cultivated land redline" is upheld during development.

Results

Spatiotemporal Evolution Characteristics of Ecosystem Services

1. Water Retention

The spatiotemporal distribution patterns of water retention services in the Nansi Lake Basin for the years 2000, 2010, and 2020 are illustrated in Fig. 2. Temporally, the water retention capacity exhibited a marked declining trend, decreasing from 6.06×10^8 m³ in 2000 to 5.25×10^8 m³ in 2010, followed by a pronounced drop to 1.34×10^8 m³ by 2020. Spatially, the distribution demonstrated significant heterogeneity, characterized by distinctly higher values in the eastern regions compared to the western areas. High water retention values align closely with forested and grassland areas, as these ecosystems effectively intercept and store surface runoff while regulating infiltration and evaporation. In contrast, urban built-up areas, dominated by impervious surfaces, consistently exhibited the lowest water retention values.

2. Soil Conservation

A comprehensive analysis of the spatial distribution characteristics reveals that the overall pattern of soil conservation capacity remained largely consistent

between 2000 and 2020. Regionally, soil conservation levels were relatively low in the central water bodies, while higher values were observed in the northeastern part of the basin, which features relatively higher terrain. The northeastern region, with its mosaic distribution of forest and grassland, high vegetation coverage, and low human activity, exhibited stronger soil conservation capacity. In contrast, the western part of the basin has experienced rapid expansion of construction land, coupled with low vegetation cover and high intensity of human activities, resulting in diminished soil retention. Water areas exhibit relatively low soil retention services due to weaker soil adhesion and a lack of vegetation for soil stabilization. Furthermore, the predominance of forest and grassland vegetation with higher coverage and limited human activity in this region contributes to enhanced soil retention.

3. Water Purification

The total nitrogen and phosphorus outputs in the Nansi Lake Basin were quantified for 2000–2020 using the InVEST model (Table 1). TN outputs were 7.82×10^6 kg (2000), 8.18×10^6 kg (2010), and 6.07×10^6 kg (2020), while TP outputs were 1.77×10^6 kg, 1.78×10^6 kg, and 1.29×10^6 kg, respectively. This represents a net decrease

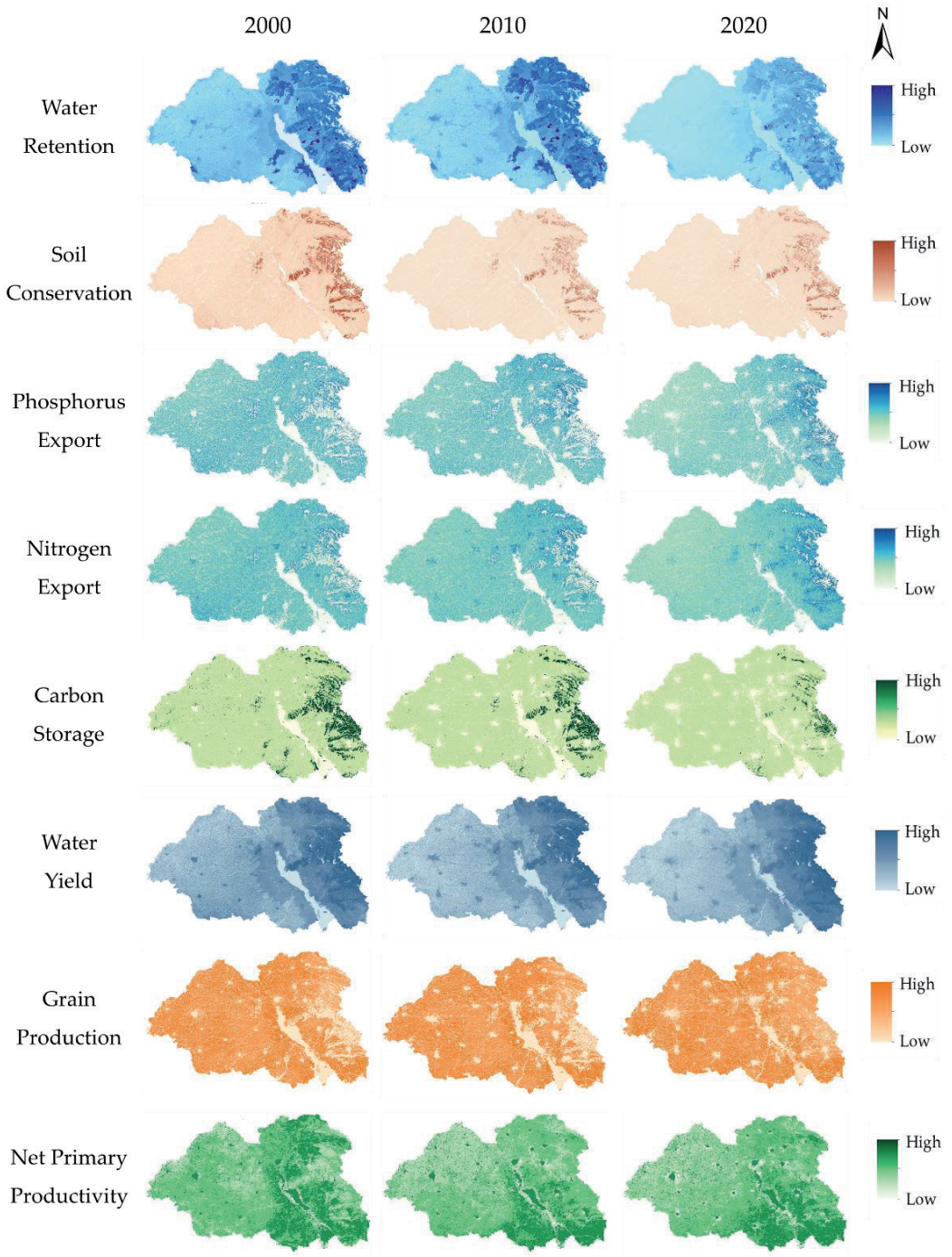

Fig. 2. Shifts in the spatiotemporal changes in seven ecosystem services in the Nansi Lake Basin (2001-2020).

Table 1. Total Nitrogen (N) and Phosphorus (P) export statistics in the Nansi Lake Basin.

Year	2000	2010	2020
Total N Output (kg)	7.82×10^6	8.18×10^6	6.07×10^6
Total P Output (kg)	1.77×10^6	1.78×10^6	1.29×10^6

of 1.75×10^6 kg in TN and 4.8×10^5 kg in TP, indicating a slight improvement in water purification capacity over the two decades. Spatially, nutrient exports were elevated in the southern region and northeastern urban areas, correlating with urban expansion, industrial activity, and population density. In contrast, forest and grassland areas exhibited lower nutrient exports due to effective vegetation retention. The basin's overall high nutrient levels are influenced by its dense river network and the proximity of residential areas to waterways, facilitating pollutant transport.

4. Carbon Storage

Carbon storage in the Nansi Lake Basin was assessed for 2000, 2010, and 2020 using the InVEST model. The results show an overall downward trend, with a total decrease of 1.3×10^6 kg. Spatially, the lowest storage occurred in water bodies, while the highest values were distributed in the northeastern forests and grasslands, confirming their high capacity. Values were also relatively high in parts of southern Xuzhou. As detailed in Table 2, carbon storage in cropland showed a pattern of initial decrease followed by an increase, while forest land, grassland, and unused land all experienced gradual declines. This decline is primarily attributed to the conversion of these land types to construction land. Across land use types, carbon storage ranked as: cultivated land > construction land > grassland > forest land > water bodies > unutilized land. The general decline was characterized by initial stability followed by a decrease linked to urban expansion, while cropland carbon storage remained stable.

5. Water Yield

The water yield of the Nansi Lake Basin was assessed for 2000-2020 using the InVEST model. The results show a clear decreasing trend, with the total water yield declining from 98.85×10^8 m³ in 2000 to 80.62×10^8 m³ in 2020, representing an overall reduction of 18.23×10^8 m³. Spatially, the distribution was characterized by higher values in the east and lower in the west, a pattern that remained relatively stable over the study period. This declining trend, as also highlighted in the 2021 Ecological Restoration and Protection Plan for the basin, underscores the impact of rapid urbanization and the pressing need for enhanced ecosystem conservation.

6. Grain Production

Based on NDVI data for cropland areas, grain production in the Nansi Lake Basin from 2000 to 2020 was estimated by multiplying the ratio of grid values to total NDVI values by the total grain output of the study area. Spatially, grain production levels generally follow a west-high, east-low pattern. High-yield areas are concentrated in the plains surrounding the Four Lakes. The western plains, with their relatively flat terrain and fertile soils, provide favorable natural conditions for crop growth. In contrast, the eastern regions exhibit more undulating topography with extensive forest and grassland areas, resulting in comparatively lower grain yields. The study area's total grain production reached 11.96 million tons in 2000, increased to 13.79 million tons in 2010, and peaked at 16.45 million tons in 2020. This continuous growth can be attributed to improvements in crop cultivation techniques and significant enhancements in production efficiency.

7. Net Primary Productivity

The spatial distribution reveals a discernible shift of high-value areas from the eastern to the southern regions, while low-value zones are concentrated in the western plains, collectively forming an east-high-west-low spatial pattern. Both forested and grassland areas exhibit relatively high NPP values, a result of a combination of factors, including higher elevation, abundant water resources, and more favorable conditions for vegetation growth. The vegetation NPP in the Nansi Lake Basin showed a slight decreasing trend over the two decades, with the average value declining from 508.73 gC/m² in 2000 to 410.39 gC/m² in 2020. Overall, the Nansi Lake Basin exhibits distinct spatial heterogeneity in NPP, with a relatively stable spatial distribution pattern over the 20 years.

Table 2. Carbon storage statistics across different land use types in the Nansi Lake Basin.

Land Use Type	2000 ($\times10^4$)	2010 ($\times10^4$)	2020 ($\times10^4$)
Arable Land	2586.78	2541.87	2705.08
Forest Land	199.27	135.70	118.09
Grass Land	369.88	289.36	45.88
Water Areas	40.87	43.73	25.24
Construction Land	391.27	469.37	572.64
Unutilized Land	4.75	3.02	0.03

Characteristics of Changes in Trade-offs and Synergies of Ecosystem Services

Weighted Synergistic Correlated Features

Pearson correlation analysis was employed to examine the trade-offs among ecosystem services in the Nansi Lake Basin from 2000 to 2020 (Fig. 3). Red cells indicate positive correlations (functional synergy), while blue cells represent negative correlations (trade-off). In 2000, carbon storage and net primary productivity showed predominantly negative correlations with several other ecosystem services, reflecting pronounced trade-offs. By 2010, the ecological tension involving carbon storage diminished, exhibiting a conflict only with water purification, while NPP maintained trade-offs with both water purification and food supply. A notable shift occurred by 2020, when carbon storage transitioned to positive correlations with all other services, indicating widespread synergies where increases in other ecosystem services were associated with rising carbon storage. The correlation between carbon storage and water yield also evolved dynamically: initially weak, it became a synergistic relationship in 2010, but reverted to a negative correlation under the combined impacts of human activities and climate change. In 2010, water purification showed strong negative correlations with both water retention and soil retention, suggesting that enhanced purification capacity occurred at the expense of these services. However, this relationship shifted to synergy in both 2000 and 2020. Water yield and soil retention maintained a synergistic relationship throughout most of the period, though it weakened over time and eventually turned negative by 2020. Both food supply and carbon storage exhibited positive correlations, with these relationships strengthening over time. As population growth and economic development increased food demand, some regions overexploited water resources to boost grain production, impairing water retention functions. Consequently, the relationship between food supply and water retention shifted from synergy to trade-off. In summary, ecosystem services exhibited dynamic and often divergent temporal trends in their pairwise interactions over the study period.

Trade-off Intensity of Ecosystem Services

This study further quantifies the intensity of trade-offs among the aforementioned ecosystem services using the RMSE indicator (Fig. 4). Overall, the coupling strength intensity among ecosystem services in the Nansi Lake Basin exhibits significant spatial heterogeneity. The trade-off intensity between water retention and water purification/carbon sequestration is generally low, suggesting potential for synergistic development and stable ecosystem growth. Minimal-tension zones for the water retention-carbon sequestration relationship are mainly distributed in the eastern part of the study area, which is characterized by relatively high elevation and dense vegetation that retains moisture and enhances carbon cycling, thereby mitigating trade-offs. The tension between water retention and grain production displays a distinct west-high-east-low pattern, with the interference index in the western region reaching values as high as 0.6. This can be attributed to intensive human activities such as construction land expansion, which has encroached on farmland, reducing grain production and imposing pressure on water retention functions. The trade-off between water retention and net primary productivity is generally subdued, with only sporadically distributed high-value areas in the eastern part of the basin. In contrast, the degree of mismatch between carbon storage and net primary productivity was generally elevated, exhibiting a decreasing gradient from east to west, with high-value areas predominantly concentrated in the eastern region. The spatial distribution pattern of interaction intensity between grain production and carbon storage/water purification was similar, with low-value areas primarily concentrated in the eastern part of the study area. Overall, the trade-

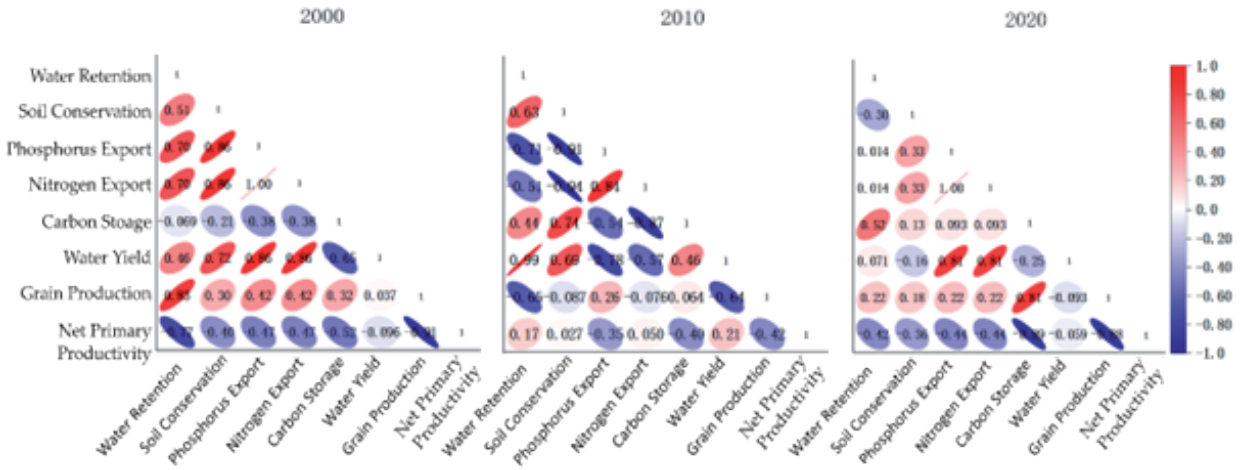

Fig. 3. Correlation coefficients of ecosystem services in the Nansi Lake Basin, 2000–2020.

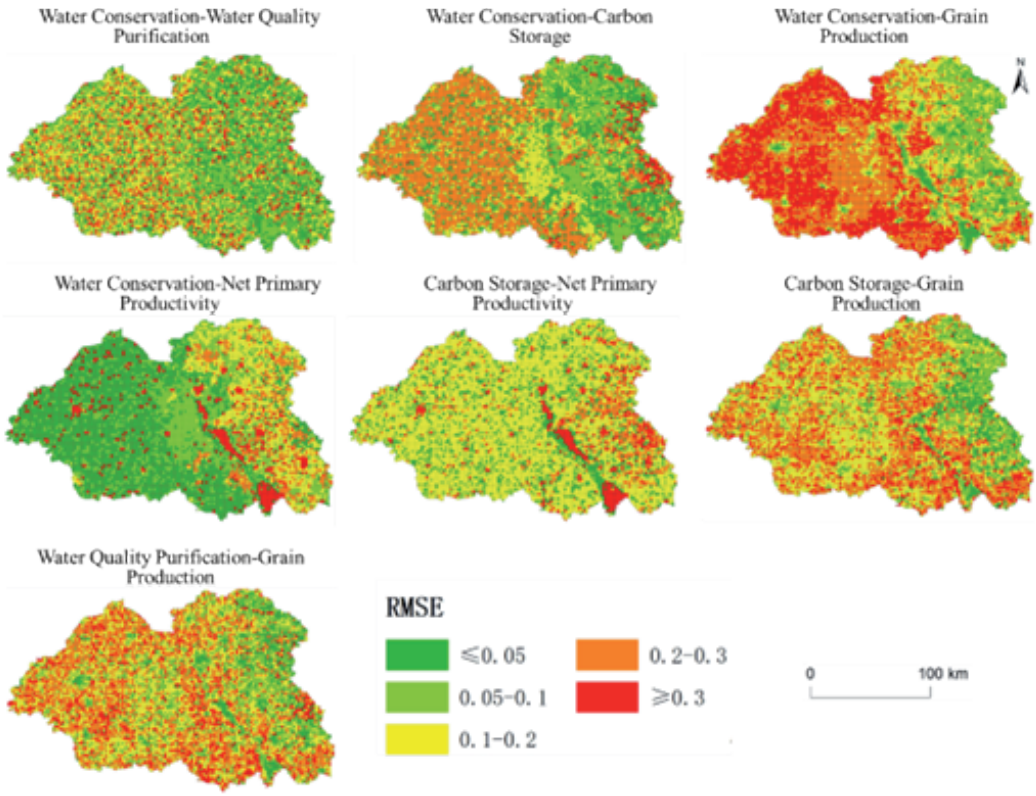

Fig. 4. Spatial variation of trade-off intensity in the Nansi Lake Basin.

off between carbon storage and water purification was relatively pronounced.

Analysis of Factors Affecting Trade-offs

Based on the actual conditions of the Nansi Lake Basin and incorporating relevant research, nine influencing factors affecting the spatial distribution of service linkages were identified from both natural and social perspectives [47]. These factors span four dimensions: climate, topography, vegetation, and socioeconomics. Specifically, they include slope (x1), annual mean temperature (x2), annual mean precipitation (x3), elevation (x4), evapotranspiration (x5), human footprint index (x6), normalized difference vegetation index (x7), per capita GDP (x8), and population density (x9). A random forest model was used to rank the relative importance of these drivers in influencing ecosystem service trade-offs in the study area, with results presented in Fig. 5. The top three most significant factors affecting these inter-service balances were selected. The GWRF model was subsequently applied to analyze the spatial heterogeneity of their importance (Fig. 6).

Evapotranspiration is the most influential factor in shaping the trade-off relationship between water retention and water purification, followed by socioeconomic indicators represented by per capita gross domestic product (GDP), while elevation modulates water retention capacity by influencing regional precipitation patterns. Per capita GDP acts as a socioeconomic indicator, while elevation modulates water retention by affecting regional precipitation. Overall, the trade-off coupling between water retention and water purification is primarily influenced by natural factors. Spatially, evapotranspiration exerts a stronger impact in the western part of the study area, particularly in Heze City. The influence of per capita GDP is most pronounced in northeastern Jining and southwestern Heze, while Zaozhuang experiences relatively weaker impacts. Elevation exerts its strongest influence in the southern region of Jining.

Water retention and carbon storage are primarily influenced by annual precipitation, elevation, and evapotranspiration. Annual precipitation significantly impacts water retention by directly regulating surface runoff and soil moisture content, which are closely linked to vegetation growth and carbon storage. Elevation affects climatic conditions and vegetation distribution, thereby influencing water retention and carbon storage. Evapotranspiration affects soil moisture and plant transpiration, playing a key role in the carbon cycle and directly contributing to carbon storage. Additionally, factors like annual mean temperature and normalized vegetation index significantly influence vegetation coverage and growth. In water retention, these elements intercept precipitation and enhance infiltration; in carbon storage, they fix carbon through photosynthesis. The intensity of the trade-off between water retention and carbon storage is highly sensitive to

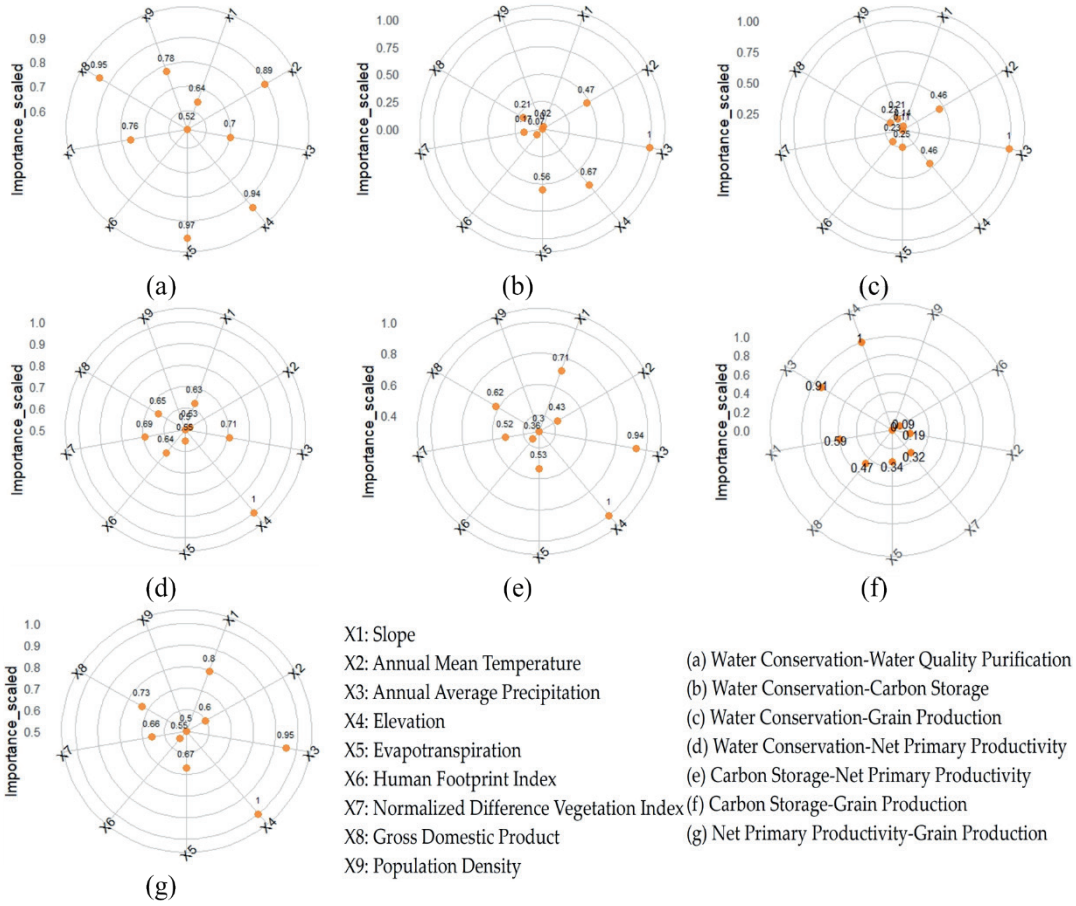

Fig. 5. Ranking of driving factors by importance in the Nansi Lake Basin.

environmental variations. Annual precipitation exerts a dominant influence on this relationship across the central and eastern parts of the study area, with the northern region experiencing lower influence. Elevation has greater influence in the low-lying water bodies and the western areas, while the eastern region remains relatively uniform in spatial influence across the entire study area.

Regarding the trade-off between water retention and grain production, annual precipitation is particularly crucial for water retention, as it directly determines farmland irrigation conditions and consequently affects crop growth and yield, which in turn shapes the observed trade-off. Elevation indirectly regulates water retention levels by affecting climate and vegetation, thereby influencing grain varieties and production volumes. Annual mean temperature significantly modulates crop growth cycles and nutrient cycling, while exerting a profound influence on the dynamic balance between water retention and grain production. Socioeconomic factors such as per capita GDP, human footprint index, and population density shape the trajectory of both services through land-use changes and agricultural development. Thus, both natural and socioeconomic factors jointly and interactively govern the competitive trade-off between water retention and grain production.

Regarding the spatial distribution of the importance of factors affecting water retention and grain production, the eastern region of the study area exhibits relatively low influence from annual precipitation, while the southern and western regions show a stronger influence. The impact of elevation is primarily distributed across the central and western parts of the study area, with Weishan County being the most affected region. High-value zones for the influence of annual mean temperature are concentrated in the southeastern part of the study area.

Elevation emerges as the most critical driver, significantly influencing both services by exerting selective pressures on climate, soil, and vegetation distribution within the study area. Annual precipitation ranks second in importance, followed by the NDVI. Annual precipitation is directly linked to water retention, while NDVI reflects vegetation coverage and growth status, influencing photosynthetic efficiency. Spatially, the central-western part of the study area is more affected by elevation and annual precipitation, while the eastern part is less affected. Central Jining and Zaozhuang are predominantly low-value zones. NDVI exhibits more pronounced influence across the Nansi Lake Basin, with higher impact areas concentrated in Heze, Xuzhou, and Tai'an.

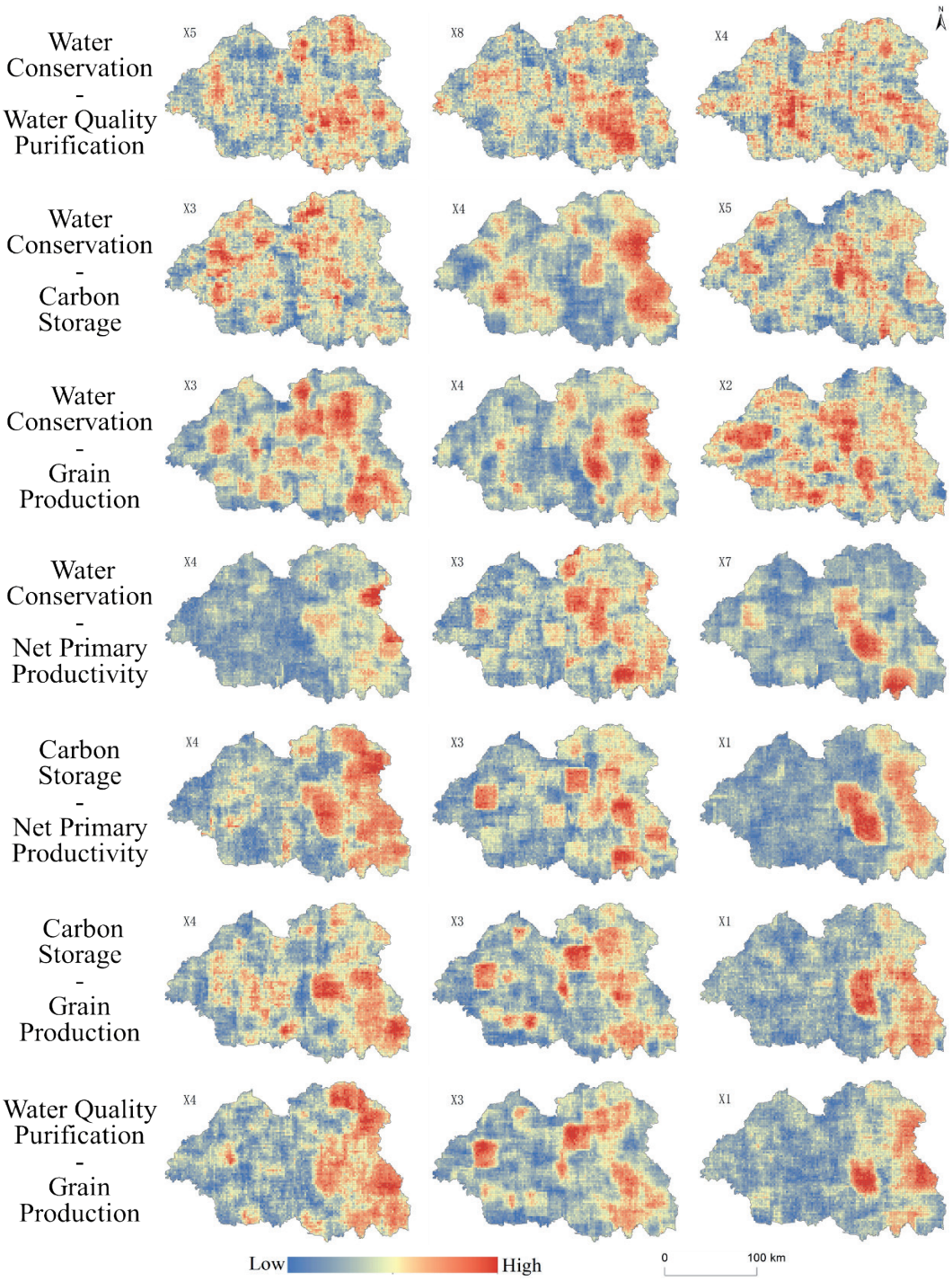

Fig. 6. Spatial distribution map of the importance of driving factors for ecosystem service trade-offs in the Nansi Lake Basin.

In the analysis of driving factors shaping the spatial trade-off between carbon storage and net primary productivity, the top three factors ranked by importance were elevation, annual precipitation, and slope. Elevation and slope influence vegetation distribution and climate variability. Different vegetation types and soil properties exhibit varying carbon storage capacities, while climate conditions also affect vegetation water use efficiency. Precipitation serves as a vital water source for vegetation growth, with adequate moisture promoting vegetation development and thereby enhancing net primary productivity. The spatial distribution of drivers underlying the trade-off between carbon storage and net primary productivity reveals significant spatial heterogeneity. The highest values for slope, annual precipitation, and elevation were recorded in Pei County. Overall, the influence pattern is relatively concentrated, primarily affecting the central-southern part of the study area.

In the ranking of driving factors for carbon storage and grain production, elevation, annual precipitation, and slope exert the strongest influence. Annual

precipitation directly determines grain crop growth and, by regulating soil moisture, also safeguards carbon accumulation. Elevation and slope jointly shape the spatial distribution of climate, soil, and vegetation, thereby indirectly regulating both ecosystem services. While higher elevations may constrain grain production, they favor long-term carbon storage. Socioeconomic factors indirectly influence both services through changing resource demands and land use patterns. Spatially, each factor exhibits distinct distribution patterns, with impacts predominantly concentrated in southeastern Zaozhuang, while the western region experiences the least influence. Slope, elevation, and annual precipitation affect broader areas, with their impacts generally decreasing from south to north.

Elevation, annual precipitation, and slope exert a profound impact on the spatial trade-off between water purification and grain production. This indicates that high vegetation coverage not only reduces pollutant entry into water bodies but also provides the necessary ecological environment for grain production, significantly impacting both. Elevation and annual precipitation also indirectly influence both through their effects on topography, climate, and hydrology. Concurrently, the Human Footprint Index exerts significant influence: human activities exert substantial pressure on water purification, yet technological improvements can enhance grain yields in agricultural production. The importance of these three factors increases progressively from northeast to southwest, with the eastern regions exhibiting the least influence. Elevation and slope exert greater impacts in the central-western parts, while annual precipitation more strongly affects the central region.

Multi-Scenario Simulation of Ecosystem Services

Using the FLUS model and actual land use data from 2000 and 2020, we simulated the spatial patterns of land use under three different development scenarios for the Nansi Lake Basin in 2040 (Fig. 7).

Under the Natural Development Scenario (NDS), significant changes in land use spatial patterns are projected. Cultivated land area is expected to decrease, with portions being converted to forest land, construction land, and other uses. Grassland distribution becomes more fragmented, with its presence primarily concentrated in the eastern part of the study area. Driven largely by the conversion of farmland and forest land, construction land expansion is particularly pronounced, especially in the central region and along river corridors. Water bodies and unutilized land show minimal changes. Under the Ecological Protection Scenario (EPS), greater emphasis on environmental conservation results in distinct forest land aggregation and expansion in the eastern study area. Farmland continues to maintain a relatively widespread distribution. Compared to other scenarios, changes in construction land are relatively minor, with grassland distribution remaining fragmented. As shown in Fig. 7, land use distribution in the Nansi Lake Basin exhibits limited variation under the Economic Development Scenario (EDS). Due to factors such as urban expansion and agricultural restructuring, portions of farmland are converted to other land uses, leading to a reduction in the size and connectivity of farmland patches. These reductions are concentrated near water bodies and construction land areas, resulting in an overall decrease in farmland density. Some forest and grassland areas have decreased due to environmental changes or human activities. Construction land has expanded significantly, facilitating urbanization in previously undeveloped areas and substantially increasing the total built-up area.

Analysis of Ecosystem Service Changes under Different Scenarios

Under the three distinct land use scenarios projected for 2040, five key ecosystem services were quantitatively assessed. The evaluation results are visually summarized in Fig. 8, with more detailed numerical changes provided in Table 3. Across the three scenarios, ecosystem services exhibited clearly divergent trends.

In the natural development scenario for 2040, ecosystem services generally demonstrated synergistic and progressive development, with relatively low trade-off intensities between services. Water retention services maintained the 2020 spatial distribution pattern of higher

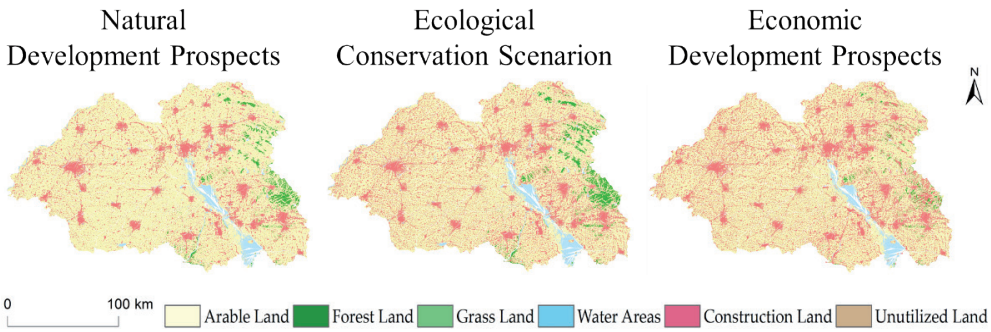

Fig. 7. Land use scenarios for the Nansi Lake Basin in 2040.

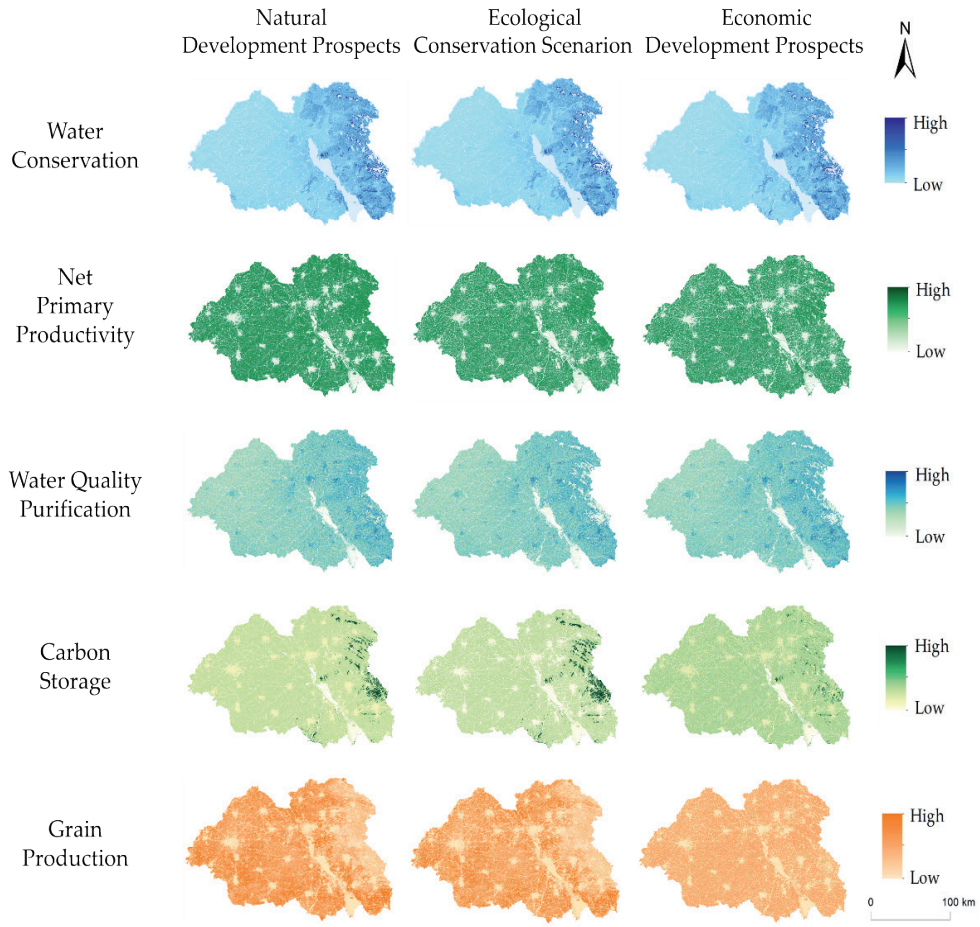

Fig. 8. Assessment of ecosystem services in the Nansi Lake Basin under different land use scenarios in 2040.

Table 3. Statistical summary of ecosystem service evaluation for the Nansi Lake Basin under different land use scenarios in 2040.

Land Use Type	Natural Development Scenario	Ecological Protection Scenario	Economic Development Scenario
Water retention (mm)	119.19	107.92	109.05
Net Primary Productivity (gc/m²)	952.95	854.56	894.05
Water Purification (10^6 kg)	7.73	7.97	7.66
Carbon Storage (10^4 t)	35.34	33.94	34.80
Grain production (10^4 t)	1845	1983	1627

values in the east and lower in the west, performing better than in the other two scenarios. This indicates that water retention services are more adaptable to natural development, effectively enhancing vegetation coverage and soil and water retention. Net primary productivity also remained high, significantly exceeding levels in both the Ecological Protection Scenario and Economic Development Scenario, indicating relatively stable energy fixation and material production capacities under natural development. Water purification services reached 7.73×10^6 kg, while carbon storage amounted to 35.34×10^4 t, reflecting the relative stability of both services under this scenario and their effectiveness in maintaining regional water quality and carbon sequestration. Land use patterns in this scenario are reasonably balanced, preserving sufficient agricultural space while sustaining ecosystem stability, thereby providing a solid natural foundation for grain production. Consequently, grain production levels are higher than in the economic development scenario but slightly lower than in the ecological conservation scenario. By reducing human interference, the natural development scenario follows ecosystem laws, resulting in relatively stable ecosystem services that synergize effectively.

The ecological conservation scenario prioritizes ecological development, achieving better restoration and protection of the environment with overall high service levels. Water retention capacity shows an

overall increase, supported by improved vegetation conditions, demonstrating the positive role of ecological conservation in sustaining water sources, soil stability, and vegetation health. Net primary productivity remains moderate due to ecological safeguards maintaining basic material and energy stability. Simultaneously, vigorous ecological conservation accelerates vegetation recovery and enhances water purification, resulting in water purification services reaching 7.97×10^6 kg – significantly surpassing the other two scenarios. Carbon storage reaches 33.94×10^4 t, while grain production peaked at 1983×10^4 tons – the highest among all scenarios. This indicates that the ecological conservation scenario not only strengthened carbon storage capacity but also mitigated conflicts between ecological protection and agricultural production to some extent. In summary, this scenario effectively safeguards multiple ecosystem services while accommodating livelihood and production needs, achieving a certain degree of synergy between ecological and economic benefits.

In contrast, under the Economic Development Scenario (EDS), the expansion of construction land and extensive vegetation loss lead to severe degradation of ecosystem services. All services perform poorly overall, with pronounced trade-offs among them. Reduced vegetation cover diminishes soil water retention capacity, thereby weakening water retention services. The disruption of ecosystem structure also severely hinders material production and energy flows, resulting in the lowest levels of net primary productivity and carbon storage among the three scenarios, particularly in areas dominated by construction land. Additionally, high-intensity human activities cause industrial and domestic pollution to exceed the self-purification capacity of water bodies, severely impairing water purification functions – water purification service output is only 7.66×10^6 kg. The substantial expansion of construction land also weakened carbon storage capacity, reaching only 34.8×10^4 t. The fossil fuel-intensive development process consumed vast amounts of fossil energy, destroyed forest vegetation, increased carbon emissions, and reduced carbon sequestration. Grain production was the lowest among the three scenarios at only 1372×10^4 t. Construction land occupied farmland and degraded soil quality, demonstrating that the single-minded pursuit of economic growth constrains agricultural production efficiency. The disorderly development under the economic growth scenario has caused multifaceted negative impacts on ecosystem services. Therefore, it is essential to seek balanced strategies that integrate economic development with ecological conservation to achieve regional sustainability.

Analysis of the Intensity of Trade-offs in Ecosystem Services under Different Scenarios in 2040

The spatial patterns of ecosystem service trade-off intensity under different scenarios by 2040 are shown in Fig. 9. The natural development scenario emphasizes the natural succession of ecosystems, where the intensity of trade-offs among ecosystem services exhibits complex spatial patterns. In this scenario, the uninterrupted natural trajectory ensures vegetation cover and biomass remain unaffected by external factors, thereby promoting water retention and purification functions to a certain extent. However, the dynamics of water resources influence the equilibrium between these two services, leading to high indices for this interaction across the basin, particularly in the eastern regions. Because this scenario avoids human interventions like land use optimization, the opportunity costs among water retention, water purification, carbon storage, and net primary productivity all increase. Scattered pockets where water purification exhibits strong trade-offs with grain production are observed throughout the study area. Conversely, the spatial distribution of trade-off intensity between water retention and grain production is generally low, with the entire basin – especially its eastern part – exhibiting relatively weak inverse relationships. Interactions associated with carbon storage remain largely stable overall, and zones with minimal trade-offs between carbon storage and grain production are widely distributed. This occurs because land use changes are slow, allowing carbon storage to benefit from natural ecosystem recovery and succession.

Under the ecological conservation scenario, which aims to protect and enhance environmental quality to maximize ecosystem service provision, the overall intensity of these trade-offs generally remains relatively high. Measures implemented to strengthen functions like water retention – such as afforestation and wetland restoration – may alter hydrological cycles and soil properties. Consequently, water retention is enhanced at a significant cost to grain production, a dynamic particularly evident in the eastern part of the study area. Increased carbon storage promotes vegetation growth and enhances the ability of plants to fix organic matter. However, heightened resource demands in the eastern region result in generally higher opportunity costs between carbon storage and net primary productivity compared to the other two scenarios, making the east a notably high-intensity zone for such interactions. By prioritizing water body protection, reducing pollutant emissions, and promoting optimized agricultural practices like green farming, this scenario creates distinct spatial differentiation, with weaker inverse effects between water purification and grain production concentrated in the eastern part of the study area.

The economic development scenario prioritizes rapid economic growth. The resulting shifts in trade-off intensities reflect the complex interplay between developmental demands and ecological conservation, necessitating careful balancing. During this process, human activities – such as intensive land utilization and large-scale infrastructure construction – drive the high-intensity exploitation of natural resources, disrupting the existing ecological equilibrium. Interestingly, the indices for water retention versus grain production,

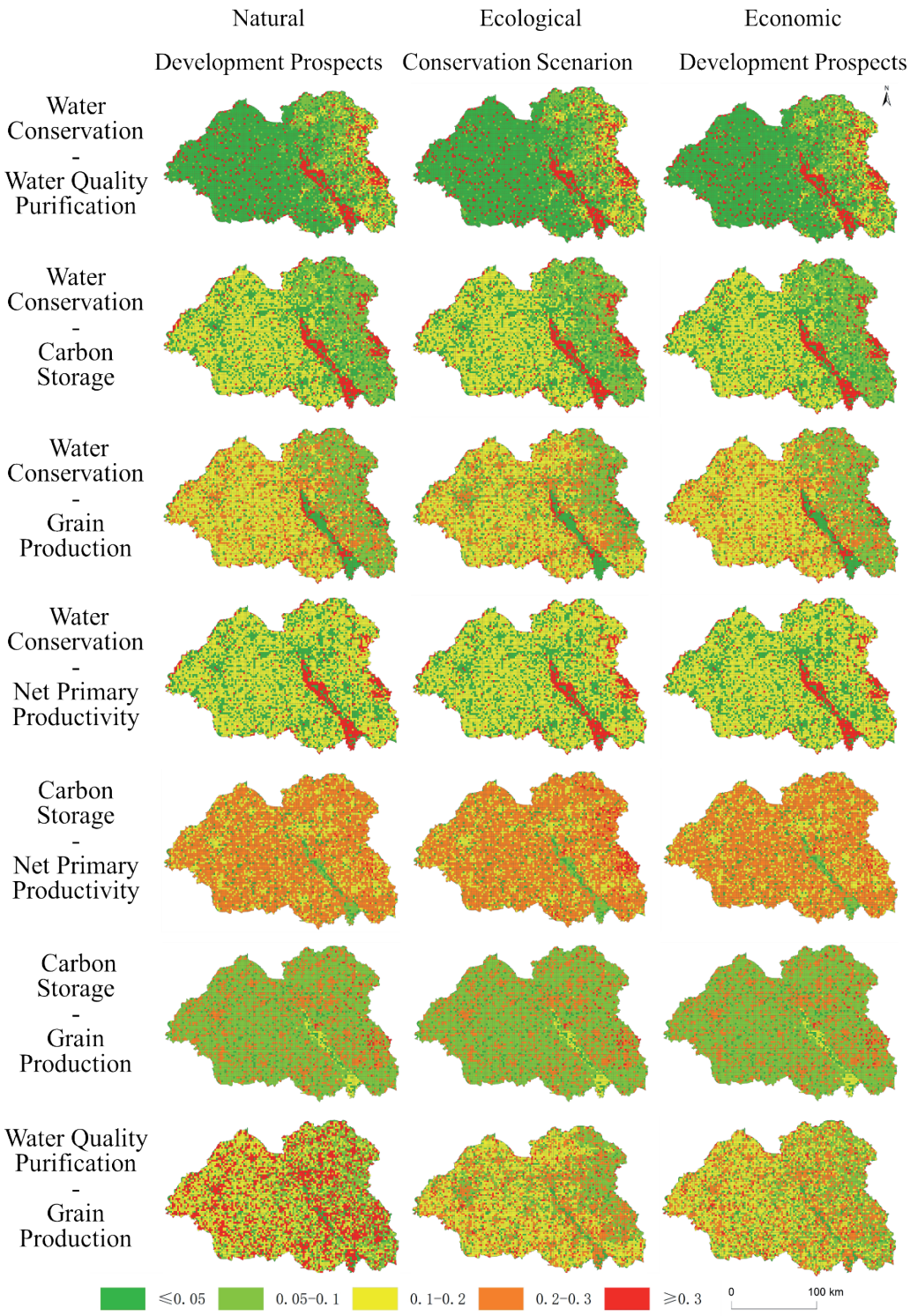

Fig. 9. Intensity of ecosystem service trade-offs under different land use scenarios in the Nansi Lake Basin by 2040.

as well as water purification versus grain production, notably diminish compared to the other two scenarios. As grain production increases substantially to meet the needs of a growing population and industry, the expansion of farmland and the overexploitation of water and carbon can cause severe ecological degradation, such as altered soil structure, soil erosion, and vegetation destruction. Despite this, in highly developed plains regions, the inverse relationships between carbon storage and grain production, water retention and net primary productivity, and water retention and carbon storage remain relatively low. Spatial distributions of water retention, water purification, and grain production exhibit lower values in the east and higher values in the west.

The varying intensity of these dynamics under three distinct development scenarios reveals crucial connections and inherent contradictions between

ecosystem services and societal development. Deepening our understanding of these trade-offs and their spatial distribution patterns can help promote economic growth while maximizing the stable provision of ecosystem services.

Discussion

Analysis of the Spatiotemporal Changes in Ecosystem Services

This study found that seven ecosystem services in the Nansi Lake Basin exhibited significant heterogeneity trends between 2000 and 2020. The soil conservation function has been declining year by year, while the total grain output and net primary productivity have continued to increase year by year. The overall trend of water purification function, carbon storage, and water production is decreasing, which is consistent with the research conclusions of Jing et al. on the Nansi Lake Basin [48]. The enhancement of water conservation capacity is related to the ecological restoration and improvement of some areas in the study area, mainly due to factors such as agricultural technological progress and planting structure adjustment [49]. The decline in carbon storage is closely related to the rapid expansion of construction land, and forest land, grassland, and other land uses are the main reasons for the decrease in carbon sink capacity [50]. However, this trend may put sustained pressure on hydrological regulation services in agricultural production. The reduction in water production and soil conservation may be influenced by the combined effects of climate change and increased human activities. These findings collectively indicate that the spatial differentiation pattern of high east and low west in the ecosystem services of the South Four Lakes and Six Lakes is influenced by multiple factors, and ecological protection is balancing the pressure of economic and social development.

Analysis of Dynamic Shifts and Intensity in Ecosystem Service Trade-offs

This study examined the spatial interactions and relationships among ecosystem services through correlation analysis and bivariate spatial autocorrelation analysis, revealing the spatial distribution pattern and dynamic evolution process of competitive intensity. Over the past 20 years, the relationship between carbon storage and other ecosystem services has shifted from opposition to synergy, while the relationship between food supply and water conservation has gradually shifted from collaboration to competition. These findings reflect the complex dynamics of ecosystem service conflicts, which is consistent with the latest research [51], suggesting that such relationships exhibit significant spatial heterogeneity when analyzed an individual-pair-bundle perspective. The trend from balancing to collaboration may indicate that over time, the positive role of regional ecological protection begins to emerge, and the restoration of ecosystems such as forests and grasslands brings about a virtuous cycle of multifunctional enhancement [52]. A multi-scale study in the Huaihe River Basin has revealed that intensified human activities have forced ecosystem services to shift from a synergistic relationship to a competitive one [53]. Overall, the conflict intensity between ecosystem services in the Nansi Lake Basin exhibits significant spatial variability.

Analysis of the Interaction between Natural and Anthropogenic Factors in Driving Trade-offs

Traditional methods [54, 55] often struggle to simultaneously consider the nonlinear relationships and spatial heterogeneity when analyzing conflict intensity, a limitation that has recently been addressed through the development of advanced integrated modelling frameworks and multi-scale analytical techniques. In contrast, the random forest model combines the advantages of geographically weighted regression and the random forest model, which can locally adapt to variable relationships and construct multiple decision trees for integrated decision-making, effectively revealing the nonlinear patterns within the data [56]. This study introduced this model for analysis and found that there are significant differences in the dominant factors and spatial effects that affect the balance between different services. The natural geographical conditions are the basis for influencing the trade-off, and the role of human socio-economic activities cannot be ignored. For example, the trade-off between food production and water conservation/carbon sequestration is influenced by both natural and socio-economic factors, which is consistent with the conclusions of previous studies [57]. By examining the interplay relationship between multiple ecosystem services, this study clarifies the reasons for the interaction between natural and human factors.

Analysis of Future Pathways Based on Multi-Scenario Simulation

The GeoSOS-FLUS model used in scenario simulation analysis comprehensively considers the impact of natural and socio-economic factors on complex land use changes, and can more accurately predict the trend of ecosystem service changes under different scenarios. This study is based on potential land use changes and uses the GeoSOS-FLUS model to simulate the conditions of the Nansi Lake Basin in three different scenarios by 2040. Under natural development scenarios, the synergistic effects between ecosystem services, such as water conservation, are significant, but the trade-off relationship in the western part of the study area has been strengthened. The ecological protection scenario demonstrates the most positive vision, while prioritizing

the protection of ecological space. The strengthening of ecological protection enhances collaborative relationships and significantly reduces trade-offs, resulting in higher levels of food production and optimal water purification functions. The economic development scenario is the most cautionary, as urbanization drives a significant expansion of construction land, exacerbating the trade-off relationship. Water conservation, net primary productivity, and carbon storage peak under the natural development scenarios, while water purification and food production perform best under the ecological protection scenarios. These findings are consistent with recent analysis by Dar et al. on a converted coastal Ramsar wetland, which emphasized that ecosystem service trade-offs are highly dependent on spatial context [58], and this study further elucidates their dynamic characteristics in the South Four Lakes Basin. Overall, the development of the Nansi Lake Basin must implement an ecological priority and green development path, and optimize the overall ecological benefits of the basin through differentiated spatial regulation.

Limitations and Future Prospects

Although this study has gained insights, there are still certain limitations. The limitations in data availability may affect the comprehensive consideration of the impact of climate change on future trends, while the exploration of the underlying mechanisms driving relationships is still insufficient. Future research can combine multidisciplinary knowledge to explore the underlying mechanisms more deeply, incorporate more variables and data, and enhance the comprehensiveness of scenario analysis. On the one hand, the evaluation of ecosystem services uses the InVEST model, and the accuracy of parameters and limitations of input data can affect the accuracy of the results [59]. On the other hand, scenario simulations only set three scenarios, but future development is influenced by various uncertain factors, such as the impact of extreme weather [60]. In the future, we can promote interdisciplinary integration, such as cross-integration with ecological economics, and provide a quantitative basis for policy development, such as ecological compensation mechanisms. This study integrates multi-source data and emerging technologies to construct a dynamic detection system for ecosystem services in the Nansi Lake Basin. Through continuous exploration of multiple disciplines and methods, the study of ecosystem service trade-offs will provide a more solid scientific basis for national spatial planning governance and ecological sustainable development.

Conclusions

This study systematically evaluated multiple ecosystem services in the Nansi Lake Basin using a phased approach: first quantitatively assessing key services, then analyzing their relationships and spatial intensity patterns, applying the GWRF model to examine differential driving effects of influencing factors, and finally projecting changes under three future scenarios. The main findings show that from 2000 to 2020, water retention capacity, grain production, and net primary productivity increased annually, while other services generally declined, all with significant spatial heterogeneity. Inter-service interactions exhibited uneven spatial distribution and complex dynamic changes, with quantitative analysis revealing pronounced spatiotemporal heterogeneity in trade-off intensity across service pairs. Dominant drivers varied, with natural factors playing a predominant role; elevation influenced productivity through climate-vegetation-soil interactions, evapotranspiration affected carbon cycling via soil-water-vegetation transpiration, and grain production was jointly influenced by natural and socioeconomic factors. Scenario-based simulations highlight distinct trade-off patterns: under natural development, farmland expansion dominates, optimizing water retention, net primary productivity, and carbon storage, with high functional mismatches for water retention and purification; under ecological conservation, forest and grassland areas increase, optimizing water purification and grain production, with generally elevated conflict intensities; and under economic development, widespread conversion to construction land results in lower trade-offs in plains areas.

Acknowledgments

This work was supported by the National Natural Science Foundation of China (Grant No. 42371307), the Ministry of Education Humanities and Social Sciences Research Project (Grant No. 24YJCZH131), the Jiangsu Province Postgraduate Research and Practice Innovation Program (Grant No. KYCX25_3180), and the Jiangsu Normal University Postgraduate Research and Practice Innovation Program (Grant No.2024XKT0108).

AI Usage Disclosure Statement

During the preparation of this manuscript, the authors used ChatGPT only for language polishing, grammar checking, and improving the clarity of English expression. The AI tool was not used for research design, data collection, data generation, data analysis, figure preparation, interpretation of results, or drawing conclusions. All AI-assisted content was carefully reviewed, revised, and verified by the authors, who take full responsibility for the content of the published article.

Conflict of Interest

The authors declare no conflict of interest.

References

1. DE GROOT R.S., WILSON M.A., BOUMANS R.M. A typology for the classification, description and valuation of ecosystem functions, goods and services. Ecological Economics, **41** (3), 393, **2002**.
2. QI B., YU M., LI Y. Multi-scenario prediction of land-use changes and ecosystem service values in the Lhasa River basin based on the FLUS-Markov model. Land, **13** (5), 597, **2024**.
3. COSTANZA R., D'ARGE R., DE GROOT R., FARBER S., GRASSO M., HANNON B., LIMBURG K., NAEEM S., O'NEILL R.V., PARUELO J. The value of the world's ecosystem services and natural capital. Nature, **387**, 253, **1997**.
4. RICHTER F.J., SUTER M., LÜSCHER A., BUCHMANN N., EL BENNI N., FEOLA CONZ R., HARTMANN M., JAN P., KLAUS V.H. Effects of management practices on the ecosystem-service multifunctionality of temperate grasslands. Nature Communications, **15** (1), 3829, **2024**.
5. REN D.-F., QIU A.-Y., CAO A.-H., ZHANG W.-Z., XU M.-W. Spatial responses of ecosystem service trade-offs and synergies to impact factors in Liaoning province. Environmental Management, **75** (1), 111, **2025**.
6. HE J.-K. Global low-carbon transition and China's response strategies. Advances in Climate Change Research, **7** (4), 204, **2016**.
7. GARCÍA-ONETTI J., SCHERER M.E., ASMUS M.L., SANABRIA J.G., BARRAGÁN J.M. Integrating ecosystem services for the socio-ecological management of ports. Ocean&Coastal Management, **206**, 105583, **2021**.
8. BENNETT E.M., PETERSON G.D., GORDON L. Understanding relationships among multiple ecosystem services. Ecology letters, **12** (12), 1394, **2009**.
9. LI C., WU Y., GAO B., ZHENG K., WU Y., LI C. Multi-scenario simulation of ecosystem service value for optimization of land use in the Sichuan-Yunnan ecological barrier, China. Ecological Indicators, **132**, 108328, **2021**.
10. WU C., WANG Z. Multi-scenario simulation and evaluation of the impacts of land use change on ecosystem service values in the Chishui River Basin of Guizhou Province, China. Ecological Indicators, **163**, 112078, **2024**.
11. JACKSON C.A., HERNANDEZ C.L., YEE S.H., NASH M.S., DIEFENDERFER H.L., BORDE A.B., HARWELL M.C., DEWITT T.H. Identifying priority ecosystem services in tidal wetland restoration. Frontiers in Ecology and Evolution, **12**, 1260447, **2024**.
12. SANTOS F., GRAW V., BONILLA S. A geographically weighted random forest approach for evaluate forest change drivers in the Northern Ecuadorian Amazon. PloS One. **14** (12), e0226224, **2019**.
13. AURET L., ALDRICH C. Interpretation of nonlinear relationships between process variables by use of random forests. Minerals Engineering, **35**, 27, **2012**.
14. CHEN Y., ZHANG R., DEHGHANIFARSANI L., AMANI-BENI M. Dynamics and Drivers of Ecosystem Service Values in the Qionglai–Daxiangling Region of China's Giant Panda National Park (1990–2020). Systems, **13** (9), 807, **2025**.
15. ZHOU Y., WEI G., WANG Y., WANG B., QUAN Y., WU Z., LIU J., BIAN S., LI M., FAN W. Estimating regional forest carbon density using remote sensing and geographically weighted random forest models: A case study of mid-to high-latitude forests in China. Forests, **16** (1), 96, **2025**.
16. XIA H., YUAN S., PRISHCHEPOV A.V. Spatial-temporal heterogeneity of ecosystem service interactions and their social-ecological drivers: Implications for spatial planning and management. Resources, Conservation and Recycling, **189**, 106767, **2023**.
17. SHENG S., HUANG J. Spatiotemporal dynamics and driving mechanisms of ecosystem services in the Beijing–Tianjin–Hebei urban agglomeration: implications for sustainable land use planning. Land, **14** (5), 969, **2025**.
18. NA L., ZHAO Y., FENG C.-C., GUO L. Regional ecological risk assessment based on multi-scenario simulation of land use changes and ecosystem service values in Inner Mongolia, China. Ecological Indicators, **155**, 111013, **2023**.
19. LI Y., PENG Y.-L., PENG H.-N., CHENG W.-Y. Assessment and multi-scenario prediction of ecosystem services in the Yunnan-Guizhou Plateau based on machine learning and the PLUS model. Frontiers in Ecology and Evolution, **13**, 1539547, **2025**.
20. HOU X., SONG B., ZHANG X., WANG X., LI D. Multi-scenario simulation and spatial-temporal analysis of LUCC in China's coastal zone based on coupled SD-FLUS model. Chinese Geographical Science, **34** (4), 579, **2024**.
21. LI Y., YAO X., LV L., LI P., LIANG J., LI H., REN S. Increasing risk of water quality deterioration in a typical inland lake of China. International Journal of Limnology, **61**, 9, **2025**.
22. YU Z., ZHAO Q. Research on the coordinated governance mechanism of cross-regional and cross-basin ecological compensation in the Yangtze River Delta. International Journal of Environmental Research and Public Health, **19** (16), 9881, **2022**.
23. LIU Y., JING Y., HAN S. Multi-scenario simulation of land use/land cover change and water yield evaluation coupled with the GMOP-PLUS-InVEST model: A case study of the Nansi Lake Basin in China. Ecological Indicators, **155**, 110926, **2023**.
24. LI Y., LIU W., FENG Q., ZHU M., YANG L., ZHANG J. Quantitative assessment for the spatiotemporal changes of ecosystem services, tradeoff–synergy relationships and drivers in the Semi-Arid Regions of China. Remote Sensing, **14** (1), 239, **2022**.
25. CHE X., JIAO L., ZHU X., WU J., LI Q. Spatial-temporal dynamics of water conservation in Gannan in the upper Yellow River Basin of China. Land, **12** (7), 1394, **2023**.
26. DEBIE E., AWOKE Z. Assessment of the effects of land use/cover changes on soil loss and sediment export in the Tul Watershed, Northwest Ethiopia using the RUSLE and InVEST models. International Journal of River Basin Management, **22** (4), 471, **2024**.
27. ABEBE W.B., DERSSEH M.G., GOSHU G., ABERA W., ABRAHAM E., MEKONNEN M.A., FOHRER N., TILAHUN S.A., MCCLAIN M.E., PAYNE W.A., BLASZCZAK J.R. Modeling changes in nutrient retention ecosystem service using the InVEST-NDR model: A case study in the Gumara River of Lake Tana Basin, Ethiopia. Ecohydrology & Hydrobiology, **25** (3), 776, **2025**.
28. KOHESTANI N., RASTGAR S., HEYDARI G., JOUIBARY S.S., AMIRNEJAD H. Spatiotemporal modeling of the value of carbon sequestration under

changing land use/land cover using InVEST model: a case study of Nour-rud Watershed, Northern Iran: N. Kohestani. Environment, Development and Sustainability, **26** (6), 14477, **2024**.
29. ZHOU Z., DING Y., LIU S., WANG Y., FU Q., SHI H. Estimating the applicability of NDVI and SIF to gross primary productivity and grain-yield monitoring in China. Remote Sensing, **14** (13), 3237, **2022**.
30. LI G., WU Z., HE Y., CHEN C., LONG Y. The promotion of sustainable land use planning for the enhancement of ecosystem service capacity: Based on the FLUS-INVEST-RUSLE-CASA model. PloS One, **19** (7), e0305400, **2024**.
31. ZHANG B., ZHENG L., WANG Y., LI N., LI J., YANG H., BI Y. Multiscale ecosystem service synergies/trade-offs and their driving mechanisms in the Han River Basin, China: implications for watershed management. Environmental Science and Pollution Research, **30** (15), 43440, **2023**.
32. LI Z., SHEN Y., FU W., QI Y., WEI X. The Spatial and temporal heterogeneity of ecosystem service trade-offs and synergies, and their implications for spatial planning and management: A case study of the Tarim River Basin. Forests, **16** (6), 1024, **2025**.
33. WU W., ZENG H., GUO C., YOU W., XU H., HU Y., WANG M., LIU X. Spatial heterogeneity and management challenges of ecosystem service trade-offs: a case study in Guangdong Province, China. Environmental Management, **73** (2), 378, **2024**.
34. JIA G., DONG Y., ZHANG S., HE X., ZHENG H., GUO Y., SHEN G., CHEN W. Spatiotemporal changes of ecosystem service trade-offs under the influence of forest conservation project in Northeast China. Frontiers in Ecology and Evolution, **10**, 978145, **2022**.
35. CONTRERAS P., ORELLANA-ALVEAR J., MUÑOZ P., BENDIX J., CÉLLERI R. Influence of random forest hyperparameterization on short-term runoff forecasting in an andean mountain catchment. Atmosphere, **12** (2), 238, **2021**.
36. GEORGANOS S., GRIPPA T., NIANG GADIAGA A., LINARD C., LENNERT M., VANHUYSSE S., MBOGA N., WOLFF E., KALOGIROU S. Geographical random forests: a spatial extension of the random forest algorithm to address spatial heterogeneity in remote sensing and population modelling. Geocarto International, **36** (2), 121, **2021**.
37. SU Z., LIN L., XU Z., CHEN Y., YANG L., HU H., LIN Z., WEI S., LUO S. Modeling the effects of drivers on PM2.5 in the Yangtze River Delta with geographically weighted random forest. Remote Sensing, **15** (15), 3826, **2023**.
38. LUO Y., SU S. SpatioTemporal Random Forest and SpatioTemporal Stacking Tree: A novel spatially explicit ensemble learning approach to modeling non-linearity in spatiotemporal non-stationarity. International Journal of Applied Earth Observation and Geoinformation, **136**, 104315, **2025**.
39. LU Z., ZHANG M., HU C., MA L., CHEN E., ZHANG C., XIA G. Spatiotemporal changes and influencing factors of the coupled production–living–ecological functions in the Yellow River Basin, China. Land, **13** (11), 1909, **2024**.
40. LIANG X., LIU X., LI X., CHEN Y., TIAN H., YAO Y. Delineating multi-scenario urban growth boundaries with a CA-based FLUS model and morphological method. Landscape and Urban Planning, **177**, 47, **2018**.
41. XING W., QIAN Y., GUAN X., YANG T., WU H. A novel cellular automata model integrated with deep learning for dynamic spatio-temporal land use change simulation. Computers & Geosciences, **137**, 104430, **2020**.
42. ZHANG M., CHEN E., ZHANG C., LIU C., LI J. Multi-scenario simulation of land use change and ecosystem service value based on the markov–FLUS model in Ezhou city, China. Sustainability, **16** (14), 6237, **2024**.
43. RANI A., GUPTA S.K., SINGH S.K., MERAJ G., KUMAR P., KANGA S., ĐURIN B., DOGANČIĆ D. Predicting future land use utilizing economic and land surface parameters with ANN and Markov chain models. Earth, **4** (3), 728, **2023**.
44. CAI G., LIN Y., ZHANG F., ZHANG S., WEN L., LI B. Response of ecosystem service value to landscape pattern changes under low-carbon scenario: A case study of Fujian Coastal Areas. Land, **11** (12), 2333, **2022**.
45. ZHANG J., LI L., LI Q., CHEN W., HUANG J., GUO Y., JI G. Multiscenario Land Use Change Simulation and Its Impact on Ecosystem Service Function in Henan Province Based on FLUS-InVEST Model. Ecology and Evolution, **15** (3), e71111, **2025**.
46. HUA H., ZHANG X., ZHOU Y., SUN J., CHEN X. Multi-scenario prediction and attribution analysis of carbon storage of ecological system in the Huaihe River Basin, China. Environmental Monitoring and Assessment, **196** (9), 814, **2024**.
47. SUN Z., LIU Y., SANG H. Spatial-temporal variation and driving factors of ecological vulnerability in Nansi Lake Basin, China. International Journal of Environmental Research and Public Health, **20** (3), 2653, **2023**.
48. JING Y., CHANG Y., CHENG X., WANG D. Land-use changes and ecosystem services under different scenarios in Nansi Lake Basin, China. Environmental Monitoring and Assessment, **193** (1), 21, **2021**.
49. PAUDEL S., GOMEZ-CASANOVAS N., BOUGHTON E.H., CHAMBERLAIN S.D., WAGLE P., PETERSON B.L., BAJGAIN R., STARKS P.J., BASARA J., BERNACCHI C., DELUCIA E.H., GOODMAN L.E., GOWDA P.H., REUTER R., SPARKS J.P., SWAIN H.M., XIAO X., STEINER J.L. Intensification differentially affects the delivery of multiple ecosystem services in subtropical and temperate grasslands. Agriculture,Ecosystems & Environment, **348**, 108398, **2023**.
50. ZHOU K., ZHENG X., HUANG S., LI H., YIN H. Quantifying the combined and individual impacts of climate and human activity on the urban green space carbon sink capacity in Beijing. Sustainable Cities and Society, **122**, 106253, **2025**.
51. AN Z., SUN C., HAO S. Spatial heterogeneity and driving forces of ecosystem services: An individual-pair-bundle perspective. Journal of Geographical Sciences, **35** (10), 2039, **2025**.
52. MARSH P., AUCKLAND S., DUDLEY T., KENDAL D., FLIES E. A mountain of health benefits? Impacts of ecological restoration activities on human wellbeing. Wellbeing, Space and Society, **4**, 100132, **2023**.
53. WANG H., ZHANG M., WANG C., WANG K., WANG C., LI Y., BAI X., ZHOU Y. Spatial and temporal changes of landscape patterns and their effects on ecosystem services in the Huaihe River Basin, China. Land, **11** (4), 513, **2022**.
54. JIN T., ZHANG P., LIU S., ZHOU N., GUO H., ZHU A.J. A novel integrated modelling framework to uncover spatial and temporal evolutionary patterns and influence mechanisms of land use conflicts. Journal of Environmental Management, **391**, 126574, **2025**.

55. WANG Y., JIANG Y., LI W., DONG S., GAO C.J. Determinants of land use conflicts with the method of cross-wavelet analysis: Role of natural resources and human activities in spatial-temporal evolution. Journal of Cleaner Production, **429**, 139498, **2023**.
56. RASHID K.J., TULI R.D., LIU W., MESEV V. Quantifying the Drivers of the Spatial Distribution of Urban Surfaces in Bangladesh: A Multi-Method Geospatial Analysis. Remote Sensing, **17** (12), 2050, **2025**.
57. QIAO J., DENG L., LIU H., WANG Z. Spatiotemporal heterogeneity in ecosystem service trade-offs and their drivers in the Huang-Huai-Hai Plain, China. Landscape Ecology, **39** (3), 42, **2024**.
58. DAR S.A., DAR J.A. Trade-offs in ecosystem services of a Ramsar wetland due to conversion into aquaculture ponds in the coastal region of Indian peninsula. Ocean & Coastal Management, **269**, 107861, **2025**.
59. RAJI S.A., ODUNUGA S., FASONA M. Spatially explicit scenario analysis of habitat quality in a tropical semi-arid zone: Case study of the sokoto–rima basin. Journal of Geovisualization and Spatial Analysis, **6** (1), 11, **2022**.
60. OTIENO T.A., OTIENO L.A., ROTICH B., LÖHR K., KIPKULEI H.K. Modeling climate change impacts and predicting future vulnerability in the Mount Kenya forest ecosystem using remote sensing and machine learning. Environmental Monitoring and Assessment, **197**, 631, **2025**.